
ELECTRON AND PHONON PROPERTIES OF PERIODIC SOLIDS VIA QUANTUM COMPUTING

DIAZ CARRAL, ANGEL

$$H = \sum_{P \in \{I, X, Y, Z\}^{\otimes n}} h_P P,$$

QUANTUM COMPUTING FOR ENGINEERS
REPORT

-
University of Stuttgart

April 12, 2022

Contents

1	Introduction	1
2	Methods	2
2.1	Wannier Tight-binding Hamiltonians (WTBHs)	2
2.2	Parametric circuit models	2
2.3	VQD	3
3	Results	3
3.1	Quantum Circuit selection	3
3.1.1	fcc-Al: Band Energy (eV) qc-calculation for Γ and X points.	3
3.1.2	cd-Si: Band Energy (eV) qc-calculation for Γ and X points. Hex-PbS: Energy vs Repetitions.	4
3.2	Electronic bandstructure	4
3.2.1	fcc-Al Bandstructure: QC vs. Classical Solver	4
3.2.2	cd-Si Bandstructure: 2 reps. vs. 6 reps.	5
3.3	Phonon bandstructure	5
3.3.1	Phonon bandstructure for fcc-Al and cd-Si.	5
4	Summary and Future Steps	6

1 Introduction

Quantum Computing for quantum chemistry and material science is one of the most promising applications because the size of Hilbert space increase linearly with the number of orbitals, compared to the classic computers where the complexity is exponential. However, noisy intermediate-scale quantum (NISQ) technologies are not yet able to solve Hamiltonians based on plane-wave basis set. There is a need to implement algorithms adapted for periodic boundary conditions of solid-state materials. Therefore, novel approaches are being developed for that purpose. In order to calculate the molecular or total energy, the PBC-adapted second-quantized Hamiltonian is mapped by Cambridge Eumen [10]. This project is focused on the electronic properties of periodic solids, which need for the electronic Hamiltonian to be computed. For that reason, the work from [2] will be followed, reproduced and extended through this report. In this paper, Wannier tight-binding functions (WTBHs)[5] in combination with Variational Quantum Eigensolver/Deflation (VQE-VQD) are applied in order to compute the bandstructure of periodic solids. In Fig.1 the qc-pipeline is depicted.

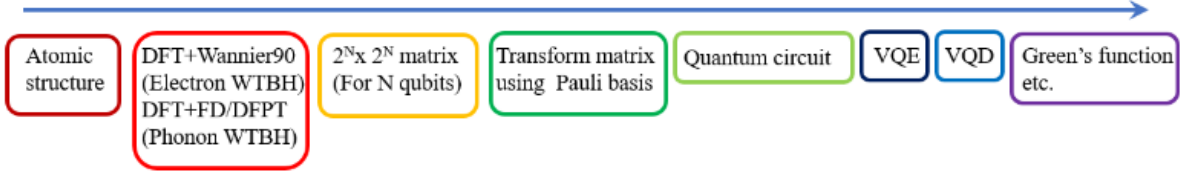


Figure 1: WTBH + VQE pipeline for the calculation of electronic properties of PBC solids [].

In this work, the energies of electric and phonon Hamiltonians for solid-state materials are accurately estimated by using WTBHs and VQD eigensolver. The results from [2] on the analysis of fcc-Aluminium are reproduced, as well as some other single-point calculations for more compounds such as Si and Ge. The qc-pipeline works as follows: First, the structure of the material is written in a POSCAR file. This is the input file for the Density Functional Theory (DFT) software VASP [8], that will generate in combination with WANNIER90 [9] the WTBHs. For simplicity, JARVIS-API [3] is called and no explicit DFT calculations are done, but instead JARVIS-WTB is used to download pre-computed WTBHs for the candidates of study. The next step is to transform the WTB functions into a $2^N \times 2^N$ Hermitian matrix, where N is the number of qubits. After that, using the *MatrixOperator()* function from Qiskit [1], the quantum circuit is stored in an Python object that will be the input for the VQD. Finally, the band energies of the material will be represented and compared to the classical numpy solver. In the next Table 1 the materials of study are shown:

Formula	JARVIS-ID	spg symbol	WTB orbitals
Al	JVASP-816	Fm-3m	8
Si	JVASP-1002	Fd-3m	16
PbS	JVASP-35680	I4/mmm	28

Table 1: List of solids analyzed by WTBH + VQD.

2 Methods

2.1 Wannier Tight-binding Hamiltonians (WTBHs)

First of all, it is mandatory to relax our candidates in order to extract the electron and phonon properties accurately from the ground state. The crystal-structures of the bulk and monolayer phases are optimized using DFT calculations in VASP with the force-field OptB88vdW. The candidates were optimized until the forces on the ions were less than 0.01 eV/Å and energy less than 10^6 eV. For the generation of WTBHs there is a tag in VASP where the user can switch the interface and connect it with WANNIER90. This last will create as an output the *wanniertbh.dat* files necessary for the next step of the qc-pipeline. The Wannier functions for a cell R and band n for a given Bloch state ψ_{nk} and unit-cell volume V are given as [2]:

$$|\mathbf{R}_n\rangle = \frac{V}{(2\pi)^3} \int \mathbf{k} e^{-i\mathbf{k}\cdot\mathbf{R}} |\psi_{nk}\rangle \psi_{nk} \quad (1)$$

We use Wannier90 to construct Maximally-Localized Wannier Functions (MLWF) based TB-Hamiltonians for electrons. For materials with magnetic properties, spin-orbit coupling was included during the calculations with VASP.

2.2 Parametric circuit models

In order to predict the eigenstates of the Hamiltonians we need to compute the output file from VASP into an Hermitian Hamiltonian matrix that can be transformed via Pauli basis in a quantum circuit. For this purpose, the module from JARVIS and Qiskit "HermitianSolver()" is used.

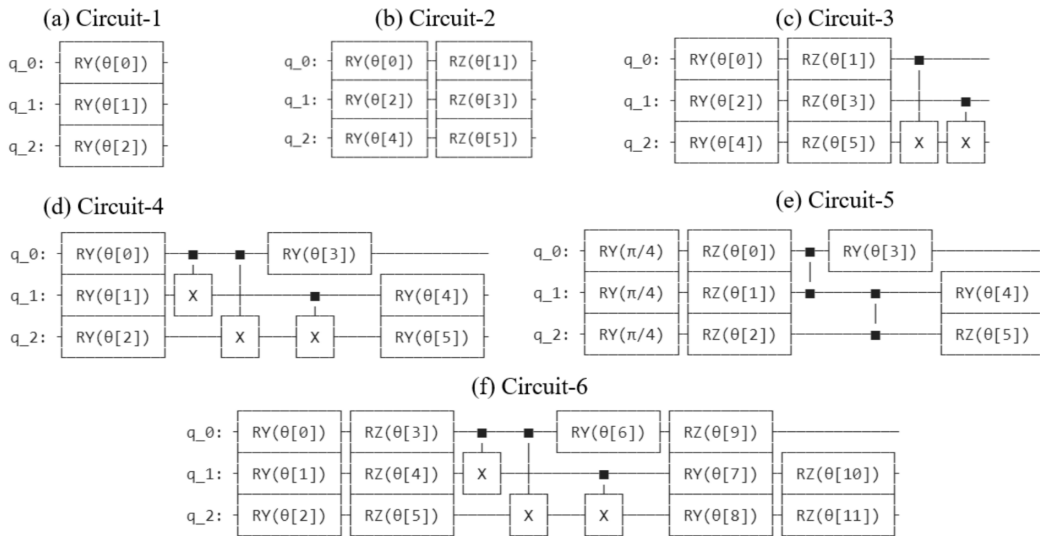


Figure 2: Set of Qiskit circuits considered for simulating fcc Al, cd Si and hex PbS. RY and RZ represent parametrized circuits with parameters θ [2]

There is a balance in the selection of parametrized quantum circuits for NISQ devices. It is important to avoid unnecessary parameters that encode redundant quantum gates. On the other hand, having and insufficient number of independent parameters can lead for the algorithm to fall in a local minima, not in the ground state.

2.3 VQD

The variational quantum deflation algorithm (VQD) is based on the combination of variation quantum eigensolver (VQE) and deflation algorithm for finding eigenvalue of a matrix. This method is one of the most straightforward ways to predict eigenstates of a Hamiltonian. In this algorithm, first, the Hermitian Hamiltonian matrix is transformed into Pauli operators. After transforming the Hamiltonian, we choose a parametrized quantum circuit and iteratively optimize so that energy expectation value for ground state is minimized. In this approach, we deflate the Hamiltonian, and perform VQE on the resultant Hamiltonian to find high energy states. The number of qubits the VQD needs is the same as the VQE, which is the main advantage in this case. The technical details about VQD can be found in [6].

3 Results

In this section the circuit optimization workflow, electronic/phonon bandstructures are shown for the materials from Table 1. All the qc-results come from the statevector simulator implemented by Qiskit.

3.1 Quantum Circuit selection

Due to the lack of an automatized code to choose the most suitable circuit for our Hamiltonian, the strategy is to run several cases involving different circuits for different repetitions of them. For example, as a first test, the band energy in the Γ point and X point of the bandstructure of fcc-Al is depicted. The number of repetitions is only equal to 1, as we are interested on the circuit which is able to approximate the eigenvalue based on the architecture only. For cd-Si we do the same test. In hex-PbS, the unit cell with the highest number of Wannier orbitals, we first select the circuit that performs best from the other previous results and then plot the energy value over the number of repetitions until the convergence appears.

3.1.1 fcc-Al: Band Energy (eV) qc-calculation for Γ and X points.

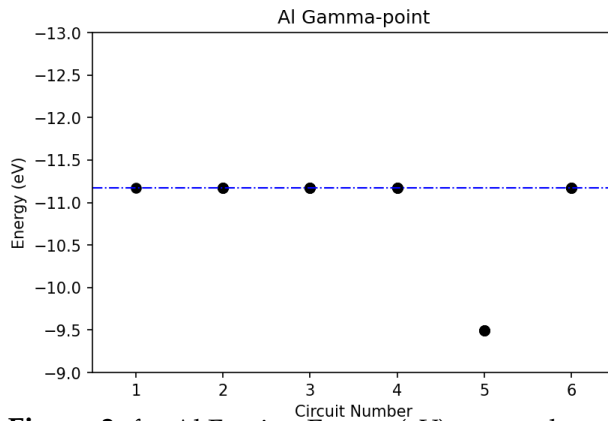


Figure 3: fcc-Al Γ point: Energy (eV) vs. number of circuit for reps = 1.

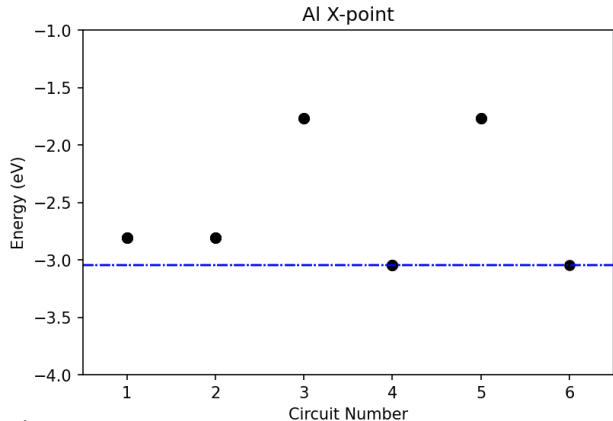


Figure 4: fcc-Al X point: Energy (eV) vs. number of circuit for reps = 1.

3.1.2 cd-Si: Band Energy (eV) qc-calculation for Γ and X points. Hex-PbS: Energy vs Repetitions.

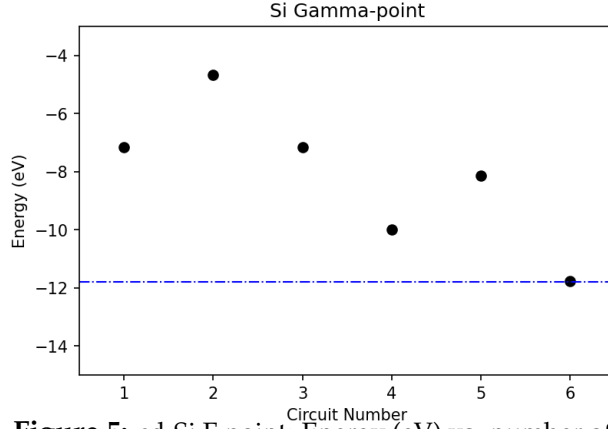


Figure 5: cd-Si Γ point: Energy (eV) vs. number of circuit for reps =1.

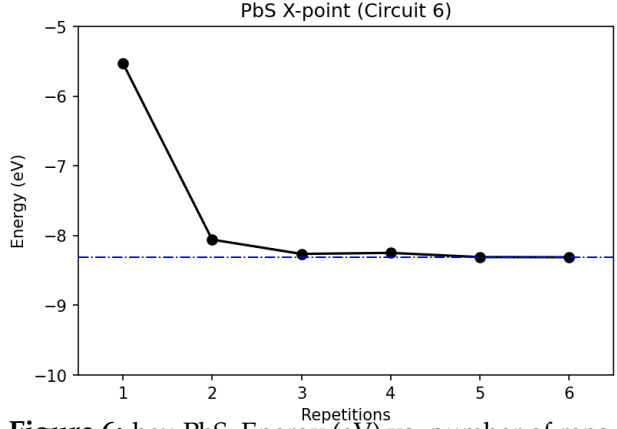


Figure 6: hex-PbS: Energy (eV) vs. number of reps. for circuit-6 "EfficientSU2".

3.2 Electronic bandstructure

In this section the electronic band structure of fcc-Al is depicted and compared with the DFT results from *materialsproject* library [7]. As a second example, there is a comparison between the QC-bandstructure of cd-Si for 2 repetitions and 6.

3.2.1 fcc-Al Bandstructure: QC vs. Classical Solver

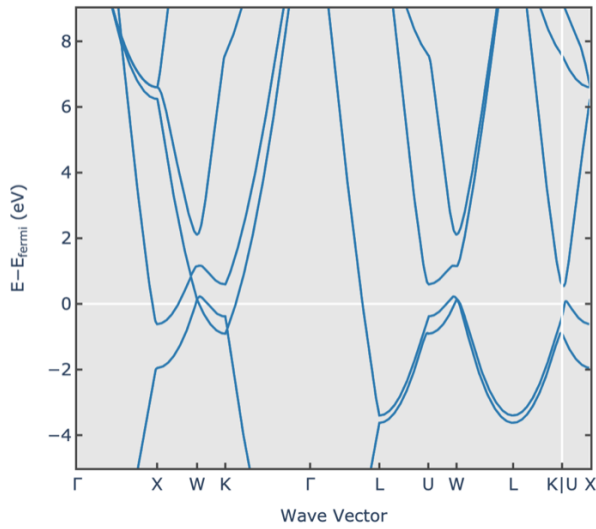


Figure 7: Interpolation for Data 1

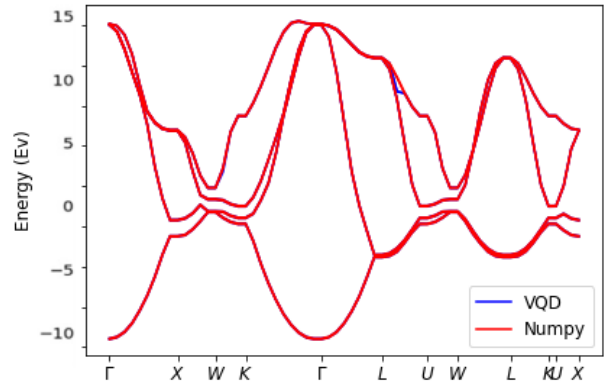


Figure 8: Interpolation for Data 2

3.2.2 cd-Si Bandstructure: 2 reps. vs. 6 reps.

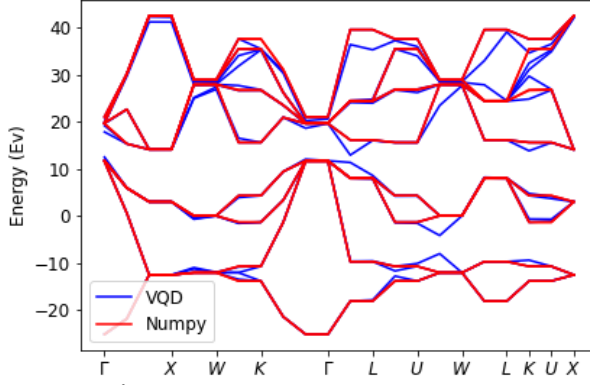


Figure 9: Interpolation for Data 1

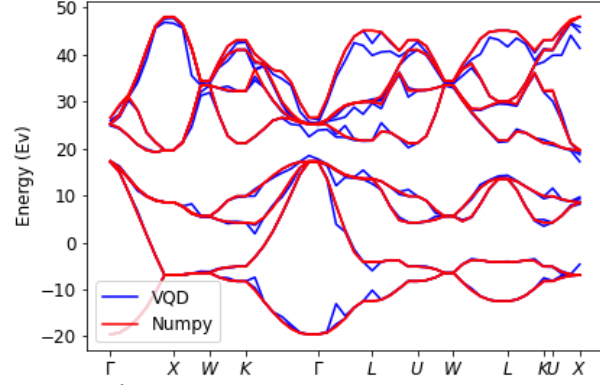


Figure 10: Interpolation for Data 2

3.3 Phonon bandstructure

The WTBHs for phonons can be obtained with finite-difference (FD) and density functional perturbation theories (DFPT) [4]. The DFPT is a well-known technique to effectively calculate the second derivative of the total energy with respect to atomic displacement. The information obtained using the DFPT method can also be utilized for predicting piezoelectric coefficients, static dielectric matrix, and Born-effective charges. The phonon Hamiltonians can also be downloaded via JARVIS-API for the same materials as the electron WTBHs.

3.3.1 Phonon bandstructure for fcc-Al and cd-Si.

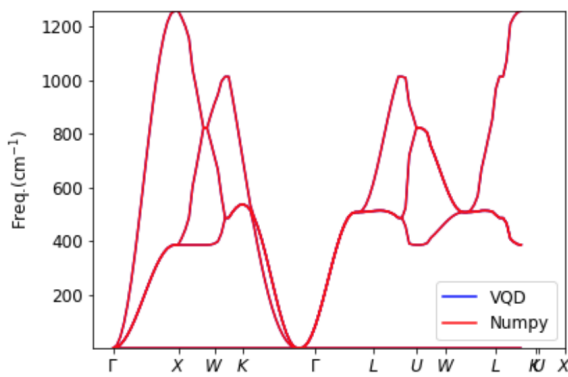


Figure 11: Phonon bandstructure for fcc-Al and reps=2

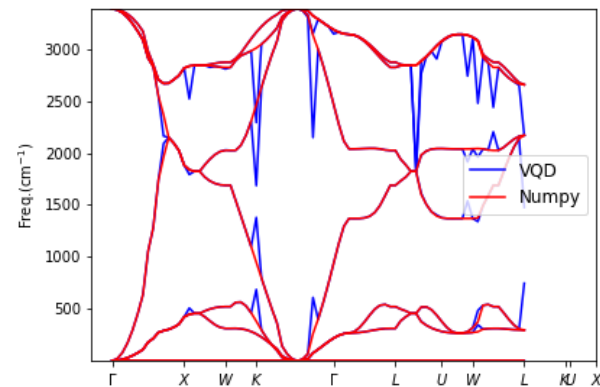


Figure 12: Phonon bandstructure for cd-Si and reps=2

4 Summary and Future Steps

In this work, the electron and phonon bandstructures of the periodic solids fcc-Al, cd-Si and hex-PbS are calculated. According to the parametrized circuit tuning, the most suitable circuit from Qiskit to perform the analysis is the circuit-6 EfficientSU2, which the Qiskit documentation proposes as “a heuristic pattern that can be used to prepare trial wave functions for variational quantum algorithms or classification circuit for machine learning.” For fcc-Al with only 8 Wannier orbitals it was easy to compute the energies only with one repetition. More complex structures such as the binary hex-PbS requires up to 6 to accurately reach the expected energy value. Same conclusions are extracted from the bandstructure, where in the case of fcc-Al the results compared to the classical numpy solver are almost same. Increasing the repetitions for cd-Si give bands closer to the expected value but also fluctuation appears over the high symmetry lines. About the phonon analysis, the results corroborate that the relaxation was successful, due to the lack of negative frequencies on the spectrum. Negatives (imaginary) frequencies give information about the unstability of the unit cell. A good relaxation should give a phonon bandstructure only on the positive side. The field of quantum computation applied to materials science and quantum chemistry opens the door to very promising new directions such as QC-accurate machine learning potentials (QMLIPs). This will be the next step that substitute the DFT-based potentials, where we take advantage of the QM domain to train a potential for MD simulations. NISQ devices and several approximations such as EUMEN or [2] will provide tools for the next years to test and compare classic MLIPs vs. QMLIPs.

References

- [1] ANIS, M. S., ET AL. Qiskit: An open-source framework for quantum computing, 2021.
- [2] CHOUDHARY, K. Quantum computation for predicting electron and phonon properties of solids. *Journal of Physics: Condensed Matter* 33, 38 (jul 2021), 385501.
- [3] CHOUDHARY, K., GARRITY, K., REID, A., DECOST, B., BIACCHI, A., HIGHT WALKER, A., TRAUTT, Z., HATTRICK-SIMPERS, J., KUSNE, A., CENTRONE, A., DAVYDOV, A., JIANG, J., PACTER, R., CHEON, G., REED, E., AGRAWAL, A., QIAN, X., SHARMA, V., ZHUANG, H., AND TAVAZZA, F. Jarvis: An integrated infrastructure for data-driven materials design, 07 2020.
- [4] CHOUDHARY, K., GARRITY, K., SHARMA, V., BIACCHI, A., HIGHT WALKER, A., AND TAVAZZA, F. High-throughput density functional perturbation theory and machine learning predictions of infrared, piezoelectric, and dielectric responses. *npj Computational Materials* 6 (12 2020).
- [5] FOULKES, W. M. C., AND HAYDOCK, R. Tight-binding models and density-functional theory. *Phys. Rev. B* 39 (Jun 1989), 12520–12536.
- [6] HIGGOTT, O., WANG, D., AND BRIERLEY, S. Variational Quantum Computation of Excited States. *Quantum* 3 (July 2019), 156.
- [7] JAIN, A., ONG, S. P., HAUTIER, G., CHEN, W., RICHARDS, W. D., DACEK, S., CHOLIA, S., GUNTER, D., SKINNER, D., CEDER, G., AND PERSSON, K. A. The Materials Project: A materials genome approach to accelerating materials innovation. *APL Materials* 1, 1 (2013), 011002.
- [8] KRESSE, G., AND HAFNER, J. Ab initio molecular dynamics for liquid metals. *Phys. Rev. B* 47 (Jan 1993), 558–561.
- [9] PIZZI, G., VITALE, V., ARITA, R., BLÜGEL, S., FREIMUTH, F., GÉRANTON, G., GIBERTINI, M., GRESCH, D., JOHNSON, C., KORETSUNE, T., IBAÑEZ-AZPIROZ, J., LEE, H., LIHM, J.-M., MARCHAND, D., MARRAZZO, A., MOKROUSOV, Y., MUSTAFA, J. I., NOHARA, Y., NOMURA, Y., PAULATTO, L., PONCÉ, S., PONWEISER, T., QIAO, J., THÖLE, F., TSIRKIN, S. S., WIERZBOWSKA, M., MARZARI, N., VANDERBILT, D., SOUZA, I., MOSTOFI, A. A., AND YATES, J. R. Wannier90 as a community code: new features and applications. *Journal of Physics: Condensed Matter* 32, 16 (jan 2020), 165902.
- [10] YAMAMOTO, K., MANRIQUE, D. Z., KHAN, I., SAWADA, H., AND RAMO, D. M. Quantum hardware calculations of periodic systems with partition-measurement symmetry verification: simplified models of hydrogen chain and iron crystals, 2022.